Dispersion characterizations and adhesion properties of epoxy composites reinforced by carboxymethyl cellulose surface treated carbon nanotubes

Dawei Zhang [a] and Ying Huang [a]*

[a] *Department of Civil, Construction and Environmental Engineering, North Dakota State University, CIE201F, 1340 Administration Ave, Fargo, ND, USA 58108*

**Corresponding author: Associate Professor, Email: ying.huang@ndsu.edu; Phone: 701-231-7651; ORCID number: 0000-0003-4119-9522*

Abstract

To improve the dispersion effectiveness of carbon nanotubes (CNTs) in epoxy and the adhesion of the resulted composites on steel substrates, this paper proposed to surface treat CNTs using carboxymethyl cellulose (CMC) in the epoxy-CNTs composite. The dispersion characterizations and adhesion properties of epoxy composites reinforced by CMC surface treated CNTs were then systematically investigated. CNTs with three different weight fractions (0.5%, 1%, and 2%) were surface treated by CMCs to improve their dispersion in epoxy-CNTs composites. It was found by Raman spectroscopy, particle size analysis, transmission and scanning electron microscopy that the CMC surface treatment was effective in reducing the size of CNT clusters to achieve a better dispersion of CNTs in such epoxy-based composite. The experimental results of contact angle and single lap joint tests indicated that better CNT dispersion resulted from the CMC surface treatment significantly improved the wettability and adhesion properties of the epoxy-CNTs composites.

Keywords: CNT-reinforced epoxy composites, CNT surface treatment, carboxymethyl cellulose, dispersion characterizations, adhesion properties

1. Introduction

Carbon nanotubes (CNTs) are allotropes of carbon with the form of cylindrical molecules [1]. The unique nanostructure of CNTs contributes to their excellent characteristics and great potentials in extensive applications which requires lightweight, high strength, electrical, and thermal conductivities. The extraordinary properties of CNTs have intrigued many research interests, and made them an ideal particle reinforcement for synthetizing polymer-matrix composite with enhanced properties and characteristics [2,3]. It is well understood that incorporating a small proportion of CNTs could considerably improve the mechanical properties of CNT-reinforced PMCs in terms of strength and toughness [4,5]. Among various polymer matrix, epoxy resin is widely recognized as one of the most favorable polymeric materials. Epoxy adhesive joints offer a great solution to join similar or dissimilar materials in structural applications due to high specific strength, uniform stress distribution, and good corrosion resistance [6,7].

A number of researches have investigated the effect of CNT addition into epoxy matrix on its mechanical properties, especially the adhesion properties [8, 9]. Literature shows that adhesion properties of epoxy composites increase as the increase of CNT proportion until a threshold (around 1%), and then decrease [10,11]. The existence of an optimal CNT proportion is mainly due to the non-uniform dispersion of CNTs in the epoxy matrix when the CNT fraction is too high [10,11]. CNTs are difficult to be uniformly and evenly dispersed in the epoxy matrix not only because of the relatively high viscosity of epoxy resin, but also owing to the extremely high aspect ratios and extremely large surface areas of CNTs, resulting in strong Van der Waals forces on the surface [12]. Without any external stimulus to break the intermodular interactions, CNTs are more likely to agglomerate and entangle into CNT clusters which normally weaken the strength, cause stress concentration and other detrimental effects as defects or imperfections [13,14]. Thus, the reinforcing efficiency of CNT-reinforced epoxy composites are highly restricted by the agglomeration and entanglement of CNTs, and a uniform dispersion has become a critical issue and a prerequisite to optimize the desired performances of CNT-reinforced epoxy composites [15,16].

Although the homogenization of CNT dispersion is still far from satisfactory, varieties of methods have been developed to promote the dispersion of CNTs into epoxy resin. Most of the prevalent methods fall into three categories: mechanical mixing, chemical, and physical surface treatments [17]. Mechanical mixing including ultrasonic mixing [18] and three-roll milling [19] is the most prevalent method to improve the dispersion by breaking up CNT clusters, but it is not able to maintain the dispersion state constantly [20]. Moreover, the disassembling process by ultrasonic methods may also cut off the length and shorten the aspect ratio of CNTs [18, 21].

On the other side, the principal mechanism of both chemical and physical surface treatments is to add soluble moieties and let them attach on the tube surface, which prevents CNTs from agglomeration [22]. Chemical treatments are usually covalent functionalization such as amino [23], silane [24], and hydroxy functionalization [25, 26], and it is proven that they are effective to modify the dispersion in practical applications [27]. However, chemical treatments could also cause structural damages on the tube walls, which in turns inevitably affects the mechanical and electrical properties of CNTs and the polymer matrix as a whole [28, 29]. Among all those methods, physical surface treatments are regarded as non-covalent functionalization with less aggressive surfactants forming physical absorption on the surface of CNTs [30, 31]. Compared to covalent functionalization, physical treatments are expected to improve the dispersion while preserving the chemical structure and original properties of the CNTs [32].

Carboxymethyl cellulose (CMC) is a water dispersible cellulose derivative, and its sodium salt has been exclusively used in food, cosmetic and pharmaceutical industries as a thicker, stabilizer or binder [33]. Recently, CMC found its new applications as a surfactant to functionalize CNTs for a better dispersion, and physical treatment using CMC is a prospective method to improve the mechanical and electrical properties of carbon nanomaterials [34, 35]. Moreover, CMC is an environmental-friendly, biocompatible, and disposable material without any harsh chemicals, which makes it even more favorable over some other solvents. However, the current application of CMC is only limited in obtaining a uniform and stabilized CNT dispersion in cementitious materials [36], no studies have incorporated CMCs into CNT-reinforced polymer materials like CNT-reinforced epoxy resin. There is a severe lack of investigations on the effect of CMC addition on dispersion state and adhesion properties of CNT-reinforced epoxy composite.

In this study, for the first time, CMC was applied to surface treat the CNTs to improve the dispersion effectiveness of CNTs in epoxy composite. The dispersion characterizations and adhesion properties of CNT-reinforced epoxy composites using CMC as a surfactant to treat CNTs were systematically investigated. For dispersion characterizations, Raman spectroscopy was carried out to prove the effectiveness of CMC treatment on the surface of CNTs. Particle size analysis was also conducted to directly reflect the dispersion state of CNTs with and without CMCs. The wettability and adhesion properties of pristine CNTs and CMC/CNT-reinforced epoxy composites were examined by contact angle test and single lap joint (SLJ) tests, respectively. In addition, transmission and scanning electron microscopy (TEM and SEM) analyses were also performed on the individual CNTs, CNT aqueous solution and CNT-reinforced epoxy composites to reveal the dispersion-modifying mechanism and result of CMCs.

2. Experimental Setup

2.1 Materials

The epoxy resin used in this study was purchased from East Coast Resin with a bisphenol A based resin and a polyamide curing agent. Multi-wall CNTs supplied by Skyspring Nanomaterials Inc were selected as the pristine CNT addition to reinforce epoxy matrix. The purity of the CNTs was more than 95%. The outside diameter, inside diameter, and length of the tubes ranged between 50-100 nm, 5-10 nm, and 5-20 μm respectively. The surfactant used in physical surface treatment was a water dispersible sodium salt of carboxymethyl ether of cellulose (sodium CMC 419273) obtained from Sigma-Aldrich Corp with formula of $C_{28}H_{30}Na_8O_{27}$ and an average mole weight around 90,000.

2.2 CMC surface treatment to CNTs

To prepare the CMC surface treated CNTs, CMCs with a constant weight fraction of 0.5% [36] were gradually added into deionized water (DI) while the solution was mechanically stirred by a magnetic rod on a magnetic stirrer at a speed of 1600 rpm. After CMCs were thoroughly dissolved in the DI water, CNTs were dispersed in the CMC solution with the same mechanical stirring. To ensure a good dispersion as well as sufficient interaction between CNTs and CMCs, the aqueous suspensions were further mechanically mixed on a tube rotator for 24h at a speed of 30 rpm. The whole mixing procedures of CNT aqueous suspensions are shown in Figure 1. The CMC surface treatment method did not involve any ultrasonic process to avoid reducing the CNT geometry and keep CNTs intact. According to the literature regarding adhesion properties of CNT-reinforced epoxy composites, around 1% was the optimal CNT fraction. As the CNT fraction got either lower and higher than 1%, bonding strength of the composites dropped accordingly [10, 11, 37]. Three different CNT fractions (0.5%, 1% and 2%) were considered to study the effect of CMCs on slightly-, mediumly- and highly-aggregated CNTs. For each CNT fraction, CNT suspensions without the CMC treatment were also prepared as the control groups.

2.3 Dispersion characterizations

The dispersion characterizations of pristine CNTs and CMC treated CNTs prepared in last section were evaluated by Raman spectroscopy and particle size analysis. Raman spectroscopy was performed using Aramis Confocal Raman Imaging Raman System, Horiba Jobin Yvon's Raman spectrometer equipped with a 532 nm laser and a 10X magnification objective lens. The recorded region was from 800 cm^{-1} to 2400 cm^{-1}. Particle size analysis was conducted using Particle Sizing Systems SPOS 780 which is capable of detecting particle sizes from 0.5 nm to 400 μm. Using DI water instead of epoxy resin as the solution for dispersion characterizations was because resin and curing agent could severely contaminate the test instruments.

2.4 Wettability

Wettability plays an important role in the adhesion properties of epoxy composites, which determines the interfacial adhesion between epoxy and substrates. The wettability of CNT-reinforced composites was measured by contact angle tests, according to ASTM D7334-08. The contact angle tests were conducted using FTA1000 Drop Shape Instrument B Frame Analyzer System. The material of the substrate was the most commonly used A36 steel (purchased from Mid America Steel Inc). Before contact angle measurements, the substrates were sandblasted and then cleaned by compressed air and sonication to remove oxide film and any foreign contaminants of the steel surfaces. The droplets were made by dispersing CNTs and CMCs following the same mixing procedures described above except the curing agent as the solution. Then the mixture was mechanically mixed with the resin at a volume ratio of 1:1. The average contact angles were obtained by measuring three droplets, and two measurements were made on the edges of each droplet.

2.5 Adhesion properties

Adhesion properties are the top priorities of the epoxy composites, especially when they are used in adhesive joints. In this study, SLJ tests were employed to determine the adhesion properties of the epoxy composites. The SLJ test specimens were designed based on ASTM D3165-07 as shown in Figure 2(a). Two adherends were bonded by epoxy adhesives at a bonding area, and two jaws were also bonded at each end of the adherends. The usage of thickened steel adherends were to prevent the specimens from early buckling before unexpected shear failure. Prior to applying epoxy adhesives, similar surface treatments were repeated on the bonding areas of all the steel sheets to obtain a good bonding performance. The thickness of the epoxy adhesives was regulated at 0.5 mm for all the specimens. The well-assembled SLJ specimens were placed in a warm room at 32 ℃ for the first 24 hours, and then the specimens were transferred to room temperature environment curing for at least seven days before testing.

SLJ tests were performed using MTS Flex Test® SE loading frame as shown in Figure 2(b). The jaws located at each end of the SLJ specimen had same thickness as the steel sheets, and they were held by the grips of the loading frame to make sure that the center line of the grips and the long axis of the SLJ specimen were coincident. Monotonic tensile loading was applied on the epoxy adhesive joints under displacement control mode at a stain rate of 1.3 mm/min until shear fracture occurred. Six different testing conditions including three CNT weight fractions (0.5%, 1%, and 2%) and two adhesive materials (pristine CNTs and CMCs treated CNTs), were involved in this study, and five specimens were prepared for each testing condition to be statistically valid. For a clear presentation of the testing conditions, the test matrix is displayed in Table 1.

3. Experimental Results and Discussions

3.1 Raman spectroscopy

Raman spectroscopy was used in this study to show the structural differences between pristine CNTs and CMCs coated CNTs. Normalized Raman spectra of pristine CNTs and CMCs coated CNTs with different CNT fractions are illustrated in Figures 3(a ~ c). As shown in Figures 3, all the spectra exhibited two main typical peaks referring to D band around 1345 cm^{-1} and G band around 1573 cm^{-1}. The locations of those two brands were consistent with the results in the literature [38, 39]. In Figures 3(c), there was another disorder-induced peak around 1607 cm^{-1} called D' band with rather weak intensity [40, 41]. It is noted that D band reflects the existence of defects, while G band represents the normal C-C bond of the carbon system [42], and the intensity ratio between D and G band, I_D/I_G is able to indicate the density of disordered structures due to any surface treatments on the CNTs [43]. The I_D/I_G ratios of pristine CNTs were 0.15, 0.24, and 0.3 for three CNT fractions of 0.5%, 1%, and 2%, respectively. After CMC treatments, the corresponding ratios increased to 0.3, 0.36 and 0.5, respectively. In terms of all CNT fractions, the increases of I_D/I_G ratios proved the effectiveness of CMC treatment indicating that CMCs were attached on the surface of CNTs and changed the physical and chemical structures of the CNTs. The attached CMCs were expected to help achieve a better CNT dispersion.

3.2 Particle size analysis

The dispersion state of CNTs depends on various factors such as type, geometry, shape and surface condition. Among all those methods to evaluate the dispersion state of CNTs, particle size analysis is the most direct ways to quantitively demonstrate the size and the distribution of CNT agglomeration. Figures 4(a ~ f) presents the particle size distributions of pristine CNTs and CMCs coated CNTs with different CNT fractions. It is obviously shown that all the particle size distributions followed an approximate normal distribution pattern, so that the average diameter is equal to the median diameter with the highest volume. As shown in Figures 4(a, c, e), The average diameters of pristine CNTs with three CNT fractions (0.5%, 1%, and 2%) were 9.4 μm, 16.3 μm, and 19.5 μm, respectively, implying that the agglomerations were more severe with higher CNT fractions. According to Figures 4(b, d, f), the average diameters of CMC treated CNTs were 7.2 μm, 8.6 μm, and 10.3 μm for the three CNT fractions, respectively. By comparing pristine CNTs and CMC treated CNTs for each fraction, the average diameters reduced significantly by 23%, 47%, and 47%, correspondingly. The results clearly indicated that large CNT clusters were broken up into smaller one with CMC surface treatment which greatly improved the dispersion states of CNTs. The particle size reduction was less significant for slightly-aggregated (0.5%) CNTs because CNTs were less likely to form CNT agglomerations with the lower fraction.

3.3 TEM analysis

The effectiveness of CMCs treatment was further illustrated by TEM analysis. The TEM observations of pristine CNTs and CMCs coated CNTs with different CNT fractions are displayed in Figures 5(a ~ f). A relatively low magnification of 0.5 μm was used to show the overall dispersion states. According to Figures 5(a, c, e), without any special dispersion methods, the dimension of those CNT clusters become larger as the increase of CNT fractions. 0.5% CNTs were only slightly aggregated, while almost all visible CNTs were entangled with 2% CNT addition. Moreover, Figures 5(a, d), (b, e) and (c, f) compare the dispersion states of pristine CNTs and CMC coated CNTs with the same fractions. For pristine CNTs, almost all of the CNTs were entangled into CNT clusters without the presence of any individual CNTs. While for CMCs coated CNTs some agglomerated CNTs were broke up into individual CNTs and the dimension of the rest

CNT clusters were apparently reduced resulting in more uniform CNT distribution states. Thus, it was evidently confirmed that CMC treatment was effective in mitigating CNT agglomerations and eventually improving the dispersion of CNTs.

To further reveal the dispersion modifying mechanism of CMCs treatment, Figures 6(a, b) present the typical TEM images of individual pristine CNTs and CMCs coated CNTs at a higher magnification. The sidewall of the pristine CNT was sharp and clear in Figure 6(a). For the CMCs coated CNTs, a thin layer was observed outside the sidewall of the CNT as shown in Figure 6(b). The boundary of pristine CNT was obviously smoother than the boundary of CMCs coated CNTs. It was directly proved that CMCs were attached on the sidewall of the CNTs forming an amorphous layer which helped build up a better CNT dispersion state.

3.4 Contact angle test

As for CNT-reinforced epoxy composites, wettability is of vital importance on the adhesion properties especially the interfacial adhesion. It is found that epoxy composite is unable to gain a solid bond without sufficient interfacial adhesion between adhesives and substrates [44]. Figures 7(a ~ f) display the appearance of CNT-reinforced epoxy droplets and their contact angles on steel substrates. As shown in Figure 7(a, b, c), the contact angle of 0.5% pristine CNT-reinforced epoxy was 44.9º. With the increase of CNT fractions to 1%, the contact angle was lowered to 43.0º indicating higher wettability and interfacial adhesion. While further adding the CNT addition to 2%, the contact angle increased to 45.1º which was even higher than the contact angle of 0.5% pristine CNT-reinforced epoxy. The CNT agglomeration might lead to the further increase of contact angle from 1% to 2% CNT fractions. CMC/CNT-reinforced epoxy showed a similar trend with the increase of CNT fractions as shown in Figure 7(d, e, f). The contact angle of 0.5% pristine CNT-reinforced epoxy came to be the highest, although epoxy composites with

1% CNT addition still yielded the best. Regarding pristine CNTs and CMC/CNT-reinforced epoxy with the same CNT additions, it is clearly observed in Figure 7(a, d), (b, e) and (c, f) that CMC/CNT-reinforced epoxy had smaller contact angles than pristine CNT-reinforced epoxy. This finding showed that CMC treatments improved the wettability of CNT-reinforced epoxy composites, and the deterioration of CNT dispersion state also had a negative influence on the wettability of the composites and interfacial adhesion at the adhesive-substrate interface.

3.5 SLJ test

Figure 8(a) presents the typical stress-strain curves of all the SLJ specimens tested in this study. All the curves shared a similar pattern with a practically linear stage followed by a nonlinear stage, while the degrees of nonlinearity varied among each curve. To compare the nonlinearities quantitively, Figure 8(b) demonstrates the areas under all the curves which are regarded as the toughness indicating the ability of plastic deformation and energy consumption. The toughness of 0.5% pristine CNT-reinforced epoxy composite was 11.56 MPa. As the CNT fractions increased to 1%, the toughness also increased to 16.58 MPa. Then when the CNT fraction continually increased to 2%, the toughness decreased to 7.3 MPa which was even lower than pristine CNT-reinforced epoxy composites with 0.5% addition. The significant decrease of toughness from 1% to 2% CNT-reinforced epoxy composites was mainly due to the formation of CNT clusters with a poor dispersion state. On the other hand, by comparing SLJ specimens with same CNT fractions but different adhesive materials, the toughness of the specimens with CMC treatments increased approximately 100%, 112%, and 338% for 0.5%, 1%, and 2% CNT fractions, respectively. It was very obvious that CMC treatments improved the toughness of CNT-reinforced epoxy composites by improving the CNT dispersion. As for the toughness of CMC/CNT-reinforced epoxy composites, although the highest value still lied in the specimens with 1% CNT addition, the lowest value went to the specimens with 0.5% addition instead of 2% addition. Since CNTs have more agglomerations with more additions, the improvements were more significant with highly aggregated CNTs.

Among all the adhesion properties of epoxy composites, the most important parameters are bonding strength and fracture strain which can be obtained from the stress-strain curve [44]. Figures 9(a, b) illustrate increments of the bonding strength and fracture strain between pristine CNTs and CMC/CNT-reinforced epoxy composites with different CNT fractions. As for pristine CNT-reinforced epoxy composites, the specimens with 1% CNT fractions gained the highest bonding strengths being 19.21 MPa, while the strengths with 0.5% fractions being 16.57 MPa which was higher than those with 2% fractions. This indicated that the precise optimal fraction lied somewhere between 0.5% and 1% (much closer to 1), and severe CNT agglomerations are more prone to occur with higher CNT fractions.

However, regarding CMC/CNT-reinforced epoxy composites, the bonding strength of the specimens with 2% CNT fraction reached 22.44 MPa, only slightly lower that the highest value of the specimens with 1% fraction being 25.43 MPa, making 0.5% fraction the worst case (20.12 MPa). Thus, the optimal fraction might get improved to the range between 1% and 2%. For comparisons between pristine and CMC/CNT-reinforced epoxy composites, it was clearly shown in Figure 9(a) that CMC treatments considerably improved the bonding strength of CNT-reinforced epoxy composites. The increments of three CNT fractions after CMC treatment reached as high as 21%, 32%, and 42%, respectively, given that the highest increments with amino or ozone functionalization reported were only around 10 ~ 15% [23, 39]. As the increase of CNT fractions, the improvements of bonding strength by CMC treatments were more and more significant. In addition, according to Figure 9(b), the variations of fracture strain were very similar to those of bonding strength, which was also consistent with the findings of toughness. The results of SLJ tests clearly showed that better dispersion states by CMC treatments had a remarkably positive effect on the adhesion properties of CNT-reinforced epoxy composites.

3.6 SEM analysis

The dispersion states of epoxy composites were further evaluated using SEM analysis to show the size of CNT clusters on the fracture surfaces. Figures 10(a ~ d) demonstrates the typical CNT clusters on the fracture surfaces of 2% pristine CNTs and CMC/CNT-reinforced epoxy composites, since most apparent differences was seen with the 2% CNT addition. For pristine CNT-reinforced epoxy composites as shown in Figure 10(a, b), there was a huge CNT cluster with a diameter of more than 21 μm on the fracture surface. The existence of that huge CNT cluster was due to that CNTs tended to form larger CNT clusters and highly aggregate with higher CNT fractions. However, for CMC/CNT-reinforced epoxy composites as shown in Figure 10(c, d), although CMC treatments did not eliminate the CNT clusters, most of the CNT clusters yielded a similar diameter around 8 μm. The remarkably smaller CNT clusters after CMC treatments were in agreement with the results of particle size analysis. Although CMC treatments did not completely break up CNT clusters into individual CNTs, it did improve the dispersion state of CNTs in the epoxy matrix by reducing the size of clusters and mitigating CNT agglomeration.

4. Conclusions

This paper introduces the use of CMC surface treatment to improve the dispersion of CNTs in epoxy-CNTs composite and investigated the dispersion characterizations and adhesion properties of the epoxy composites reinforced by CMC surface treated CNTs for three different CNTs fractions (0.5%, 1%, and 2%). The results of Raman spectroscopy and TEM analysis proved the effectiveness of CMC treatments that CMCs were attached on the surface of CNTs forming a thin amorphous layer. It was found by particle size analysis, TEM, and SEM analysis that although CMC treatments did not completely break up all the CNT clusters into individual CNTs, CNT dispersion states were improved by reducing the size of CNT clusters after CMC treatments. For 1% and 2% CNT addition, the CNT agglomerations were significantly mitigated with average diameter reductions of 47%. While the dispersion improvement was less significant for 0.5% CNT addition, since CNTs were less likely to agglomerate with a low fraction. The improved CNT dispersion state by CMC treatments also had a positive influence on the wettability and adhesion properties of CNT-reinforced epoxy composites. Due to better CNT dispersion state with CMC treatments, CMC/CNT-reinforced epoxy composites had stronger interfacial adhesion, higher toughness, bonding strength, and fracture strain compared to pristine CNT-reinforced epoxy composites.

CRediT authorship contribution statement

Dawei Zhang: Data curation, Methodology, Formal analysis, Investigation, Writing - original draft, Writing - review & editing. **Ying Huang:** Project administration, Funding acquisition, Supervision, Writing - review & editing.

Declaration of interest

The authors declare that they have no known competing financial interests or personal relationships that could have appeared to influence the work reported in this paper.

Acknowledgements

This work was supported the National Science Foundation under Grant No. CMMI-1750316. The findings and opinions expressed in this article are those of the authors only and do not necessarily reflect the views of the sponsors.

Reference

[1] S. Iijima, Helical Microtubules of Graphitic Carbon, Nature 354 (1991) 56-58. https://doi.org/10.1038/354056a0

[2] Z. Ahmadi, Epoxy in nanotechnology: A short review, Prog. Org. Coatings. 132 (2019) 445–448. https://doi.org/10.1016/j.porgcoat.2019.04.003

[3] J.N. Coleman, U. Khan, W.J. Blau, Y.K. Gun'ko. Small but strong: A review of the mechanical properties of carbon nanotube-polymer composites, Carbon N Y 44 (2006) 1624–1652. https://doi.org/10.1016/j.carbon.2006.02.038.

[4] A. Kausar, I. Rafique, B. Muhammad. Review of Applications of Polymer / Carbon Nanotubes and Epoxy / CNT Composites, Polym. – Plast. Technol. Eng. 55 (2016) 1167–1191. https://doi.org/10.1080/03602559.2016.1163588.

[5] Y. Li, Q. Wang, S. Wang. A review on enhancement of mechanical and tribological properties of polymer composites reinforced by carbon nanotubes and graphene sheet: Molecular dynamics simulations, Compos. Part B Eng. 160 (2019) 348–361. https://doi.org/10.1016/j.compositesb.2018.12.026.

[6] M.D. Banea, L.F.M. Da Silva, Adhesively bonded joints in composite materials: An overview, Proc. Inst. Mech. Eng. Part L J. Mater. Des. Appl. 223 (2009) 1–18. https://doi.org/10.1243/14644207JMDA219.

[7] D. Zhang, Y. Huang, Influence of surface roughness and bondline thickness on the bonding performance of epoxy adhesive joints on mild steel substrates, Prog. Org. Coatings 153 (2021) 106135. https://doi.org/10.1016/j.porgcoat.2021.106135.

[8] D. Zhang, Y. Huang, The bonding performances of carbon nanotube (CNT)-reinforced epoxy adhesively bonded joints on steel substrates, Prog. Org. Coatings 159 (2021) 106407. https://doi.org/10.1016/j.porgcoat.2021.106407.

[9] H. Khoramishad, M. Khakzad, Toughening epoxy adhesives with multi-walled carbon nanotubes, J. Adhes. 94 (2018) 15–29. https://doi.org/10.1080/00218464.2016.1224184.

[10] S.A. Sydlik, J.H. Lee, J.J. Walish, E.L. Thomas, T.M. Swager, Epoxy functionalized multi-walled carbon nanotubes for improved adhesives, Carbon N Y 59 (2013) 109–120. https://doi.org/10.1016/j.carbon.2013.02.061.

[11] A. Kumar, K. Kumar, P.K. Ghosh, A. Rathi, K.L. Yadav, Raman, MWCNTs toward superior strength of epoxy adhesive joint on mild steel adherent, Compos. Part B Eng. 143 (2018) 207–216. https://doi.org/10.1016/j.compositesb.2018.01.016.

[12] A. Thess, R. Lee, P. Nikolaev, H. Dai, P. Petit, J. Robert, Crystalline ropes of metallic carbon nanotubes, Science 273 (1996) 483-487. https://doi.org/10.1126/science.273.5274.483

[13] E. Gao, W. Lu, Z. Xu, Strength loss of carbon nanotube fibers explained in a three-level hierarchical model, Carbon N Y 138 (2018) 134–142. https://doi.org/10.1016/j.carbon.2018.05.052.

[14] G.D. Zhan, J.D. Kuntz, J.E. Garay, A.K. Mukherjee, Electrical properties of nanoceramics reinforced with ropes of single-walled carbon nanotubes, Appl. Phys. Lett. 83 (2003) 1228–1230. https://doi.org/10.1063/1.1600511.

[15] G. Pandey, E.T. Thostenson, Carbon nanotube-based multifunctional polymer nanocomposites, Polym. Rev. 52 (2012) 355–3416. https://doi.org/10.1080/15583724.2012.703747.

[16] G. Pircheraghi, R. Foudazi, I. Manas-Zloczower, Characterization of carbon nanotube dispersion and filler network formation in melted polyol for nanocomposite materials, Powder Technol. 276 (2015) 222–231.

https://doi.org/10.1016/j.powtec.2015.02.031.

[17] P.C. Ma, N.A. Siddiqui, G. Marom, J.K. Kim, Dispersion and functionalization of carbon nanotubes for polymer-based nanocomposites: A review, Compos. Part A Appl. Sci. Manuf. 41 (2010) 1345–1367. https://doi.org/10.1016/j.compositesa.2010.07.003.

[18] X.L. Jia, Q. Zhang, J.Q. Huang, C. Zheng, W.Z. Qian, F. Wei, The direct dispersion of granular agglomerated carbon nanotubes in bismaleimide by high pressure homogenization for the production of strong composites, Powder Technol. 217 (2012) 477–481. https://doi.org/10.1016/j.powtec.2011.11.004.

[19] H. Yang, Y. Yang, Y. Liu, D. He, J. Bai, Multi-scale study of CNT and CNT-COOH reinforced epoxy composites: dispersion state, interfacial interaction vs mechanical properties, Compos. Interfaces 28 (2021) 381–393. https://doi.org/10.1080/09276440.2020.1780556.

[20] A.H. Korayem, M.R. Barati, S.J. Chen, G.P. Simon, X.L. Zhao, W.H. Duan. Optimizing the degree of carbon nanotube dispersion in a solvent for producing reinforced epoxy matrices, Powder Technol. 284 (2015) 541–550. https://doi.org/10.1016/j.powtec.2015.07.023.

[21] K.G. Dassios, P. Alafogianni, S.K. Antiohos, C. Leptokaridis, N.M. Barkoula, T.E. Matikas, Optimization of sonication parameters for homogeneous surfactant assisted dispersion of multiwalled carbon nanotubes in aqueous solutions, J. Phys. Chem. C 119 (2015) 7506–7516. https://doi.org/10.1021/acs.jpcc.5b01349.

[22] Y.P. Sun, K. Fu, Y. Lin, W. Huang, Functionalized carbon nanotubes: Properties and applications, Acc. Chem. Res. 35 (2002) 1096–1104. https://doi.org/10.1021/ar010160v.

[23] M.D. Shokrian, K. Shelesh-Nezhad, R. Najjar, Effect of CNT dispersion methods

on the strength and fracture mechanism of interface in epoxy adhesive/Al joints, J. Adhes. Sci. Technol. 33 (2019) 1394–1409. https://doi.org/10.1080/01694243.2019.1595304

[24] Ma PC, Kim JK, Tang BZ. Effects of silane functionalization on the properties of carbon nanotube/epoxy nanocomposites. Compos Sci Technol 2007;67:2965–72. https://doi.org/10.1016/j.compscitech.2007.05.006.

[25] A. Bisht, K. Dasgupta, D. Lahiri, Investigating the role of 3D network of carbon nanofillers in improving the mechanical properties of carbon fiber epoxy laminated composite, Compos. Part A Appl. Sci. Manuf. 126 (2019). https://doi.org/10.1016/j.compositesa.2019.105601.

[26] A. Bisht, K. Dasgupta, D. Lahiri, Effect of graphene and CNT reinforcement on mechanical and thermomechanical behavior of epoxy—A comparative study, J. Appl. Polym. Sci. 135 (2018). https://doi.org/10.1002/app.46101

[27] A. Li, Z. Fang, L. Tong, A. Gu, F. Liu, Improving dispersion of multiwalled carbon nanotubes in polyamide 6 composites through amino-functionalization, J. Appl. Polym. Sci. 106 (2007) 2898–2906. https://doi.org/10.1002/app.24599.

[28] M. Monthioux, B.W. Smith, B. Burteaux, A. Claye, J.E. Fischer, D.E. Luzzi, Sensitivity of single-wall carbon nanotubes to chemical processing: an electron microscopy investigation, Carbon N Y 39 (2001) 1251-1272. https://doi.org/10.1016/S0008-6223(00)00249-9.

[29] G.L. Burkholder, Y.W. Kwon, R.D. Pollak, Effect of carbon nanotube reinforcement on fracture strength of composite adhesive joints, J. Mater. Sci. 46 (2011) 3370–3377. https://doi.org/10.1007/s10853-010-5225-6.

[30] Z. Qi, Y. Tan, H. Wang, T. Xu, L. Wang, C. Xiao, Effects of noncovalently functionalized multiwalled carbon nanotube with hyperbranched polyesters on

mechanical properties of epoxy composites, Polym. Test. 64 (2017) 38–47. https://doi.org/10.1016/j.polymertesting.2017.09.031.

[31] Y. Chen, W. Wei, Y. Zhu, J. Luo, X. Liu, Noncovalent functionalization of carbon nanotubes via co-deposition of tannic acid and polyethyleneimine for reinforcement and conductivity improvement in epoxy composite, Compos. Sci. Technol. 170 (2019) 25–33. https://doi.org/10.1016/j.compscitech.2018.11.026.

[32] J. Cha, S. Jin, J.H. Shim, C.S. Park, H.J. Ryu, S.H. Hong, Functionalization of carbon nanotubes for fabrication of CNT/epoxy nanocomposites, Mater. Des. 95 (2016) 1–8. https://doi.org/10.1016/j.matdes.2016.01.077.

[33] M.S. Rahman, M.S. Hasan, A.S. Nitai, S. Nam, A.K. Karmakar, M.S. Ahsan, et al, Recent Developments of Carboxymethyl Cellulose, Polymers (Basel) 13 (2021) 1345. https://doi.org/10.3390/polym13081345.

[34] L. Long, F. Li, M. Shu, C. Zhang, Y. Weng, Fabrication and application of carboxymethyl cellulose-carbon nanotube aerogels, Materials (Basel) 12 (2019) 1867. https://doi.org/10.3390/ma12111867.

[35] J. Fu, D. Li, G. Li, F. Huang, Q. Wei, Carboxymethyl cellulose assisted immobilization of silver nanoparticles onto cellulose nanofibers for the detection of catechol, J. Electroanal. Chem. 738 (2015) 92–99. https://doi.org/10.1016/j.jelechem.2014.11.025.

[36] L. Chia, Y. Huang, P. Lu, A.N. Bezbaruah, Surface Modification of Carbon Nanotubes Using Carboxymethyl Cellulose for Enhanced Stress Sensing in Smart Cementitious Composites, IEEE Sens. J. 21 (2021) 15218–15229. https://doi.org/10.1109/JSEN.2021.3073619.

[37] Ayatollahi MR, Nemati Giv A, Razavi SMJ, Khoramishad H. Mechanical properties of adhesively single lap-bonded joints reinforced with multi-walled

carbon nanotubes and silica nanoparticles. J Adhes 2017;93:896–913. https://doi.org/10.1080/00218464.2016.1187069.

[38] C.E. Pizzutto, J. Suave, J. Bertholdi, S.H. Pezzin, L.A.F. Coelho, S.C. Amico, Study of epoxy/CNT nanocomposites prepared via dispersion in the hardener, Mater. Res. 14 (2011) 256–263. https://doi.org/10.1590/S1516-14392011005000041.

[39] P. Jojibabu, Y.X. Zhang, A.N. Rider, J. Wang, B. Gangadhara Prusty, Synergetic effects of carbon nanotubes and triblock copolymer on the lap shear strength of epoxy adhesive joints, Compos. Part B Eng. 178 (2019) 107457. https://doi.org/10.1016/j.compositesb.2019.107457.

[40] A. Jorio, R. Saito, Raman spectroscopy for carbon nanotube applications, J. Appl. Phys. 129 (2021). https://doi.org/10.1063/5.0030809

[41] M.S. Dresselhaus, G. Dresselhaus, R. Saito, A. Jorio, Raman spectroscopy of carbon nanotubes, Phys. Rep. 409 (2005) 47–99. https://doi.org/10.1016/j.physrep.2004.10.006

[42] L. Bokobza, J. Zhang, Raman spectroscopic characterization of multiwall carbon nanotubes and of composites, Express Polym. Lett. 6 (2012) 601–608. https://doi.org/10.3144/expresspolymlett.2012.63.

[43] M. Bourchak, K.A. Juhany, N. Salah, R. Ajaj, A. Algarni, F. Scarpa, Determining the Tensile Properties and Dispersion Characterization of CNTs in Epoxy Using Tem and Raman Spectroscopy, Mech. Compos. Mater. 56 (2020) 215–226. https://doi.org/10.1007/s11029-020-09874-6.

[44] D. Zhang, Y. Huang, Y. Wang, Bonding performances of epoxy coatings reinforced by carbon nanotubes (CNTs) on mild steel substrate with different surface roughness, Compos. Part A Appl. Sci. Manuf. 147 (2021) 106479.

https://doi.org/10.1016/j.compositesa.2021.106479.

Figure captions

Figure 1. CMC and CNT mixing procedures.

Figures 2. SLJ test: (a) SLJ specimen configurations; (b) test set-up.

Figures 3 Raman spectra of pristine CNTs and CMCs coated CNTs with different CNT fractions: (a) 0.5%; (b) 1%; (c) 2%.

Figures 4 particle size distributions of pristine CNTs and CMCs coated CNTs with different CNT fractions: (a) C0.5; (b) CC0.5; (c) C1; (d) CC1; (e) C2; (f) CC2.

Figure 5 TEM observations of pristine CNTs and CMCs coated CNTs with different CNT fractions: (a) C0.5; (b) CC0.5; (c) C1; (d) CC1; (e) C2; (f) CC2.

Figures 6 TEM observations of pristine CNTs and CMCs coated CNTs at higher magnification: (a) pristine CNTs; (b) CMCs coated CNTs.

Figures 7 CNT-reinforced epoxy droplets and their contact angles: (a) C0.5; (b) C1; (c) C2; (d) CC0.5; (e) CC1; (f) CC2.

Figures 8 SLJ test results: (a) stress-strain curves of SLJ specimens; (b) Toughness of SLJ specimens.

Figures 9 Increments of the bonding strength and fracture strain between pristine CNTs and CMC/CNT-reinforced epoxy composites with different CNT fractions: (a) bonding strength; (b): fracture strain

Figures 10 Typical CNT clusters on the fracture surfaces of 2% pristine CNTs and CMC/CNT-reinforced epoxy composites: (a) C2; (b) close-view of the CNT cluster of C2; (c); CC2; (d) close-view of the CNT cluster of CC2.

Table 1 SLJ test results

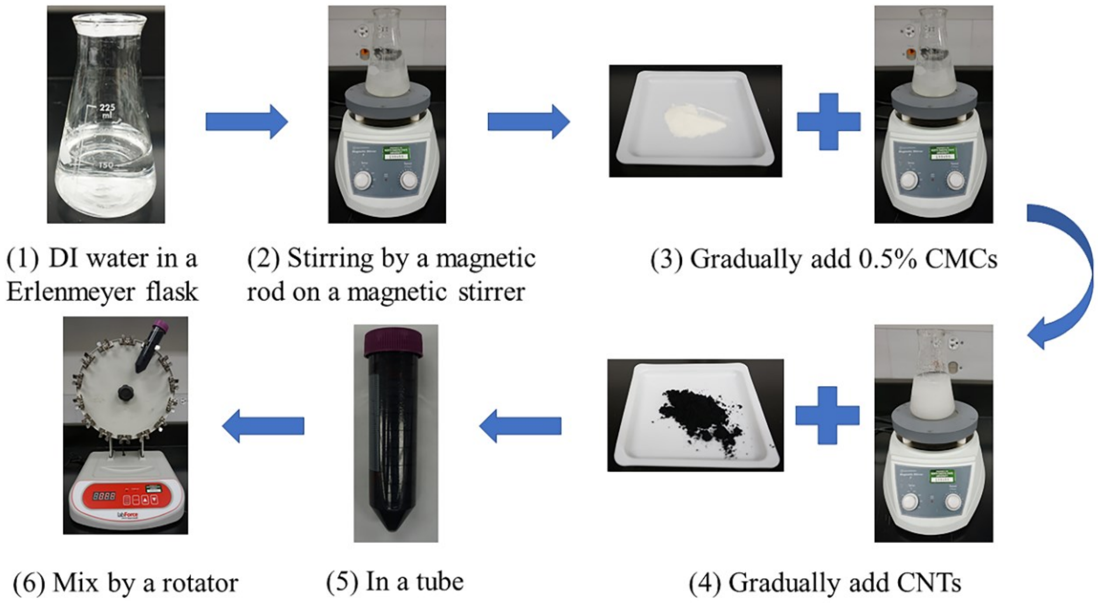

Figure 1. CMC and CNT mixing procedures

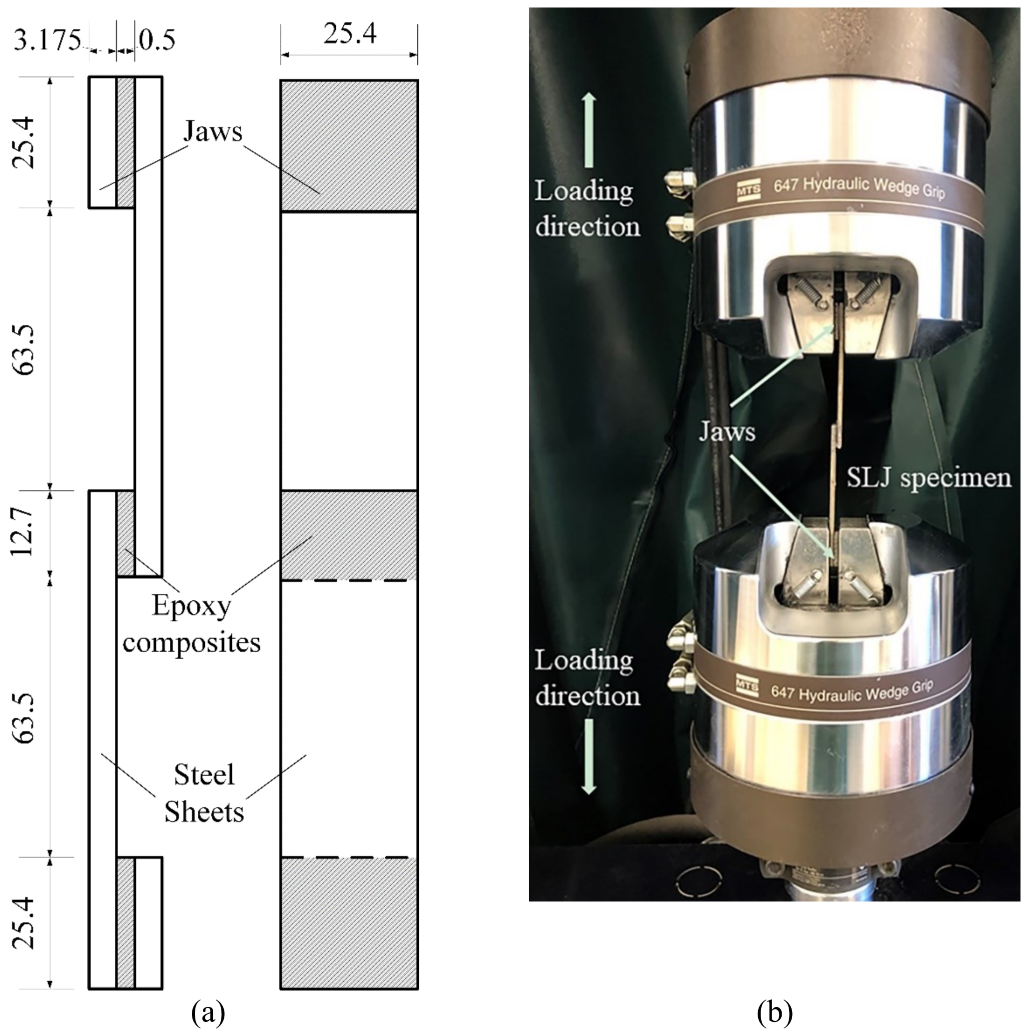

Figures 2. SLJ test: (a) SLJ specimen configurations; (b) test set-up

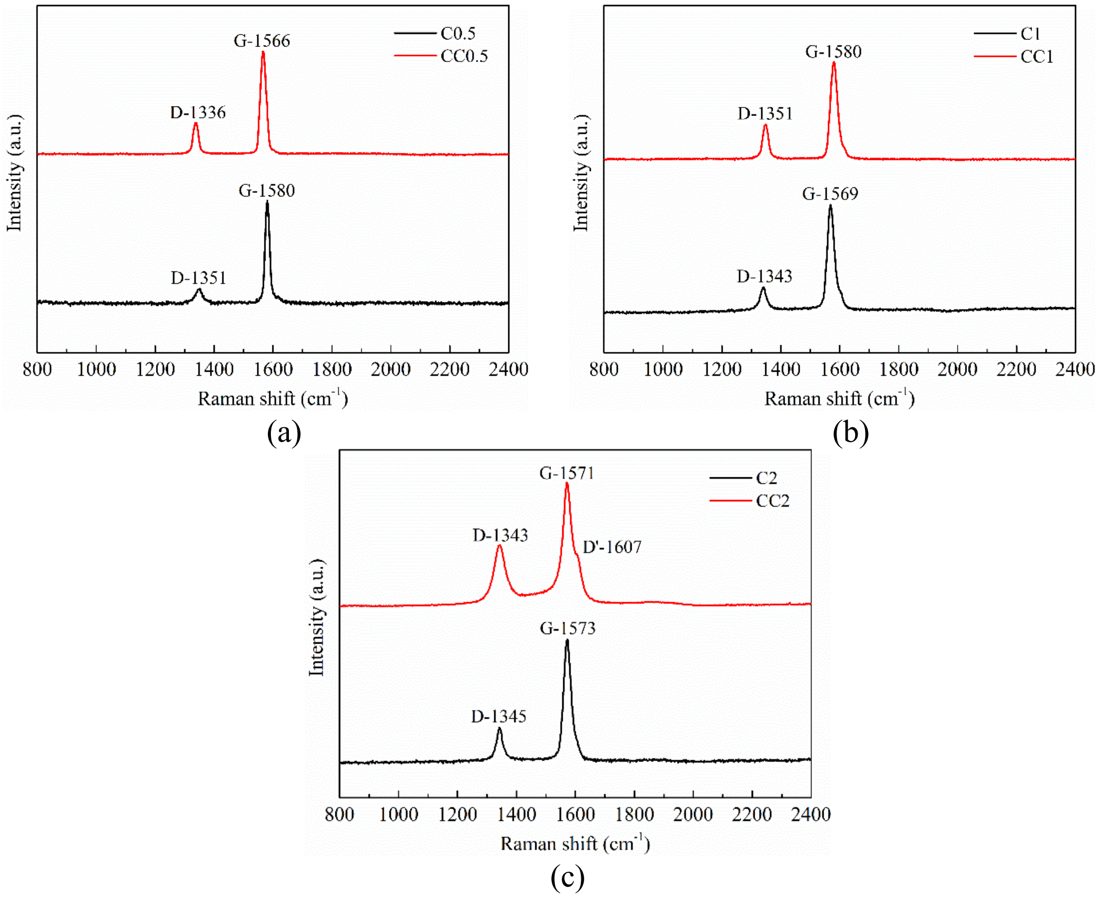

Figures 3 Raman spectra of pristine CNTs and CMCs coated CNTs with different CNT fractions: (a) 0.5%; (b) 1%; (c) 2%.

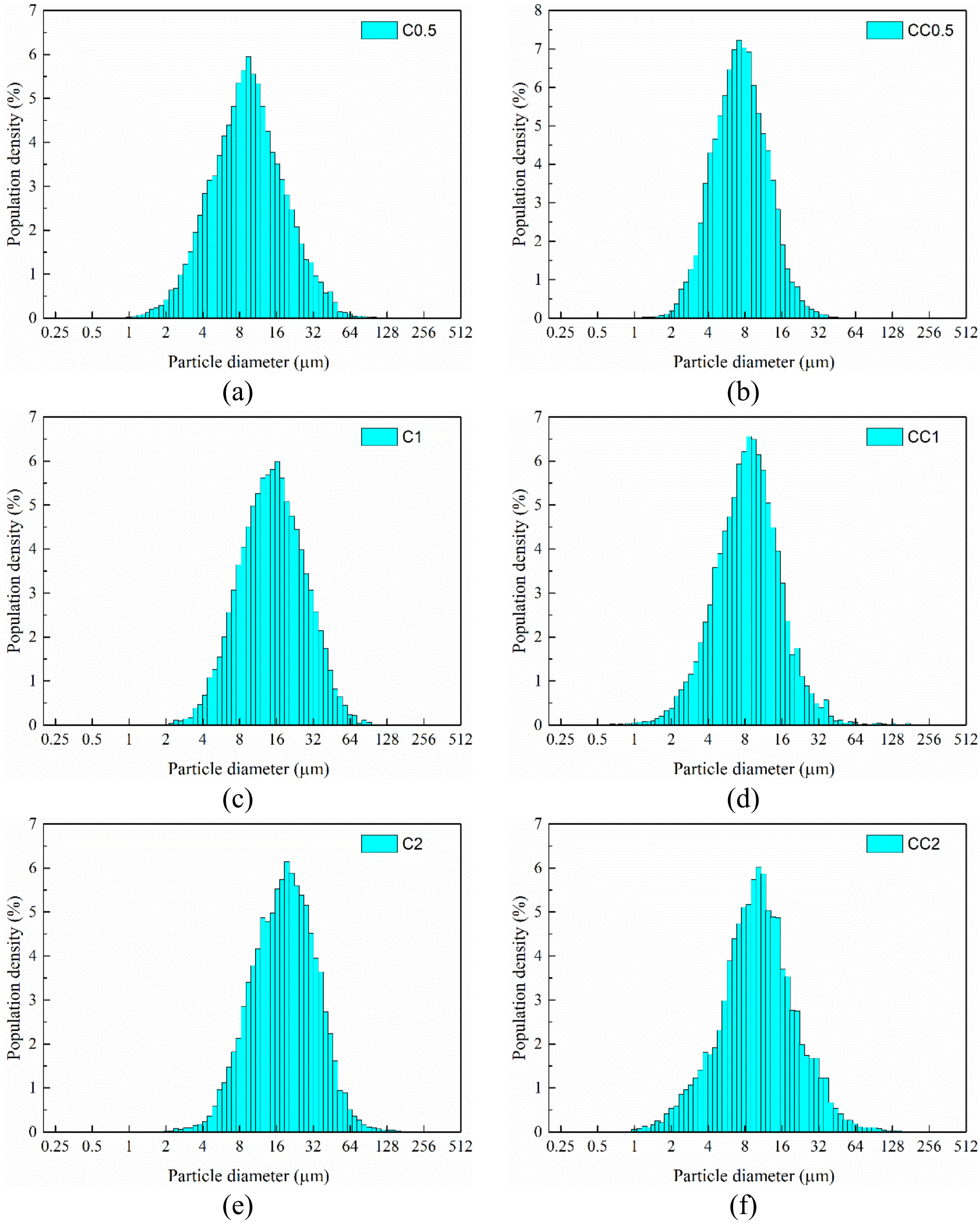

Figures 4 particle size distributions of pristine CNTs and CMCs coated CNTs with different CNT fractions: (a) C0.5; (b) CC0.5; (c) C1; (d) CC1; (e) C2; (f) CC2.

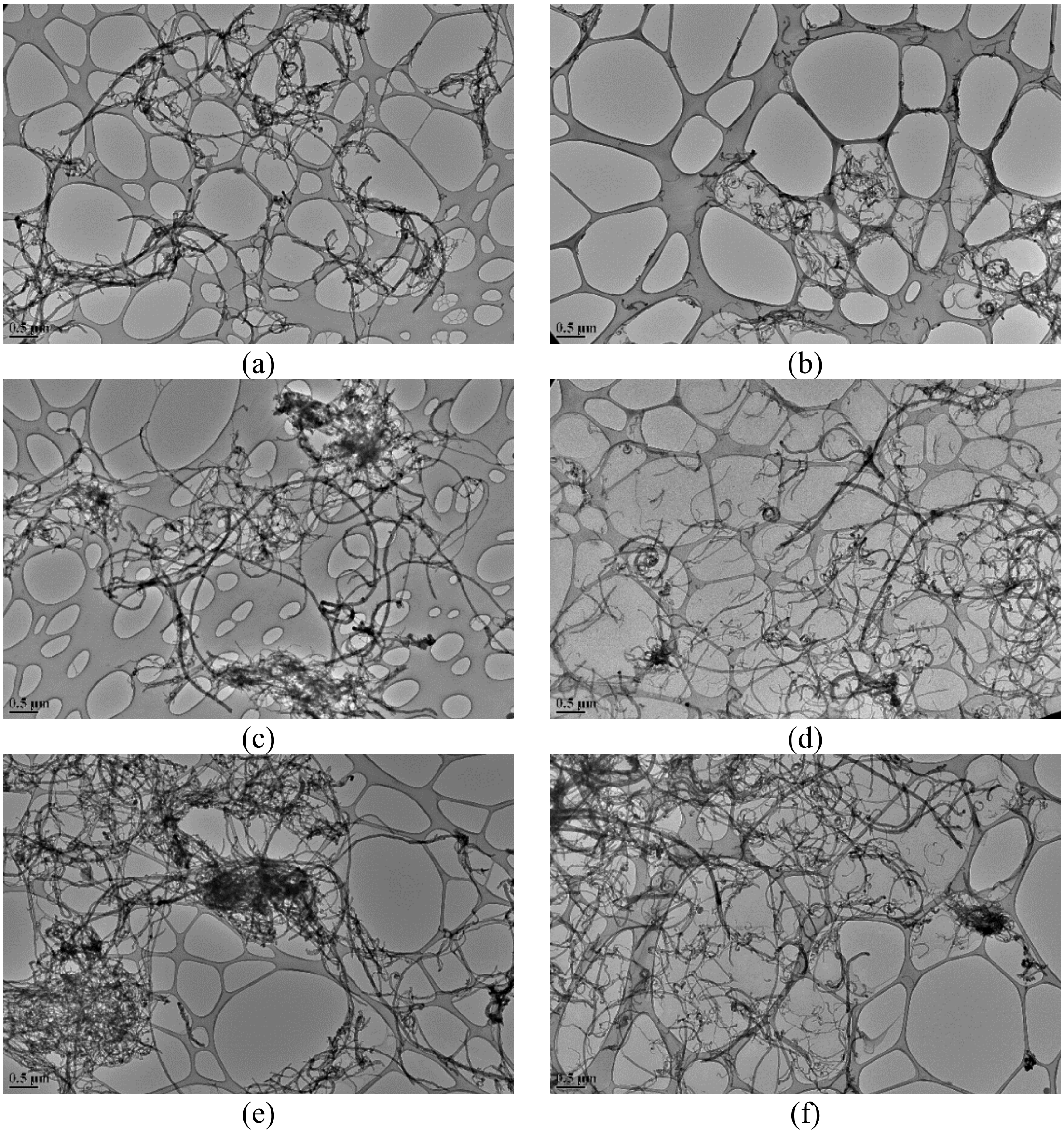

Figures 5 TEM observations of pristine CNTs and CMCs coated CNTs with different CNT fractions: (a) C0.5; (b) CC0.5; (c) C1; (d) CC1; (e) C2; (f) CC2.

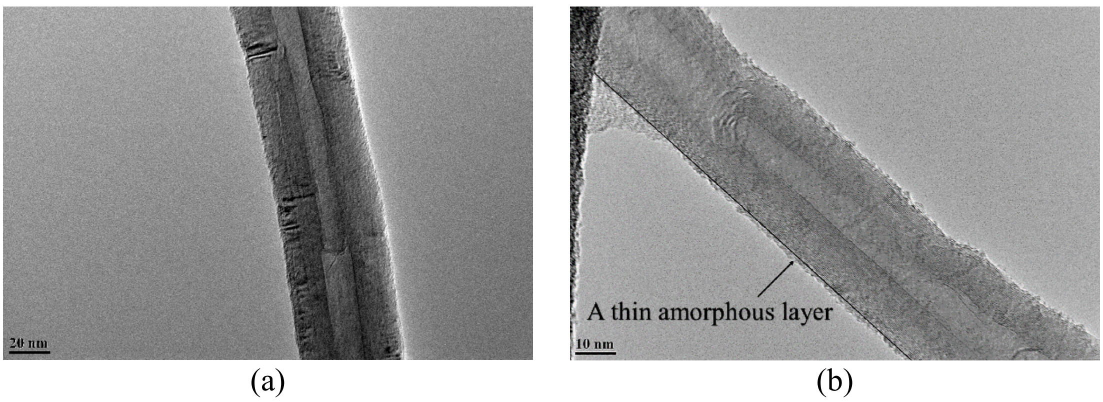

Figures 6 Typical TEM images of individual pristine CNTs and CMCs coated CNTs at a higher magnification: (a) pristine CNTs; (b) CMCs coated CNTs

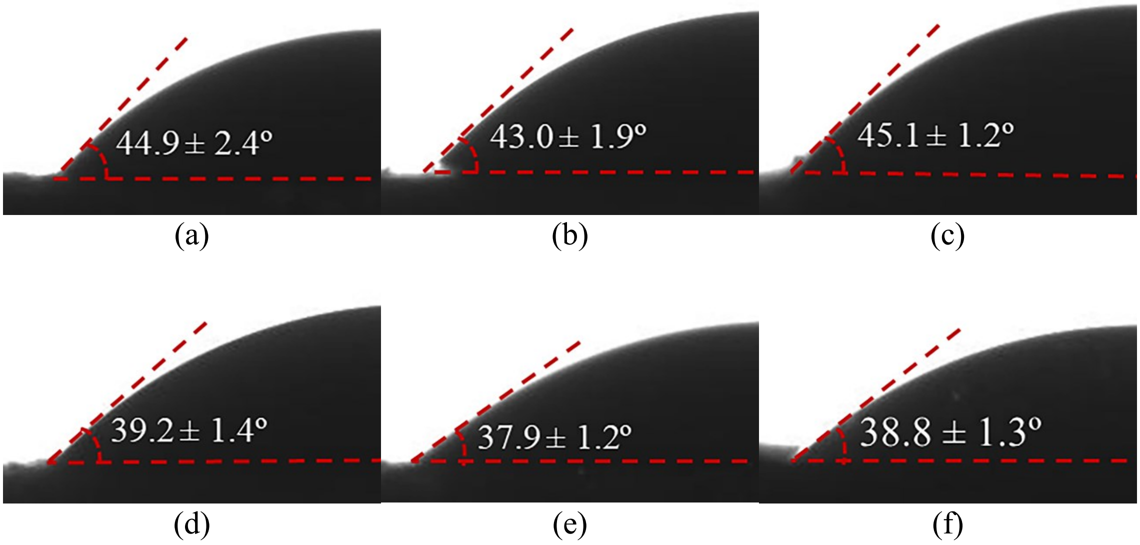

Figures 7 CNT-reinforced epoxy droplets and their contact angles: (a) C0.5; (b) C1; (c) C2; (d) CC0.5; (e) CC1; (f) CC2.

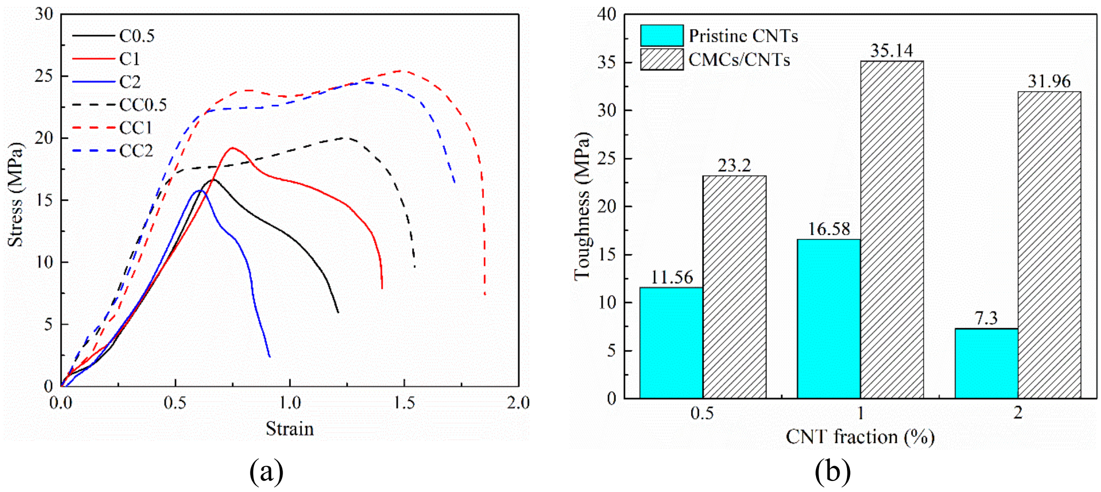

Figures 8 SLJ test results: (a) stress-strain curves of SLJ specimens; (b) Toughness of SLJ specimens.

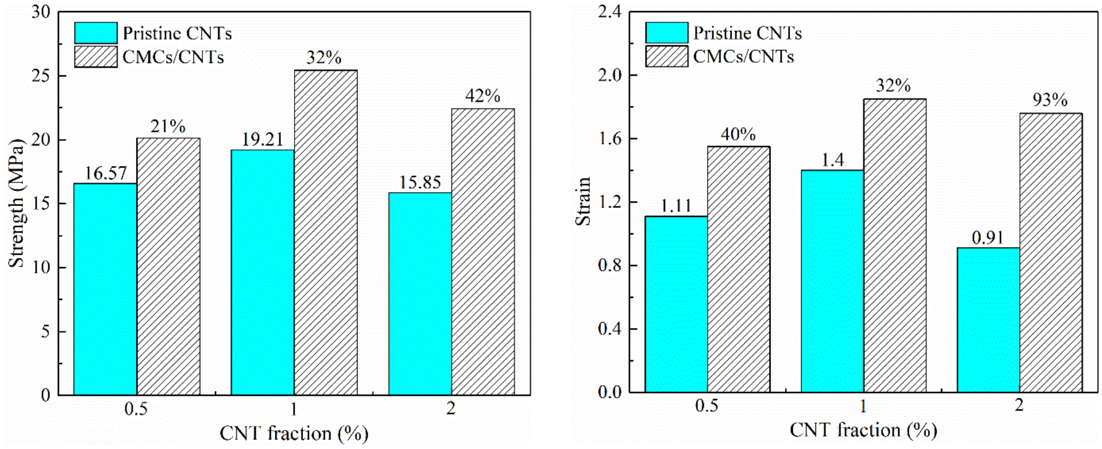

(a) (b)

Figures 9 Increments of the bonding strength and fracture strain between pristine CNTs and CMC/CNT-reinforced epoxy composites with different CNT fractions: (a) bonding strength; (b): fracture strain

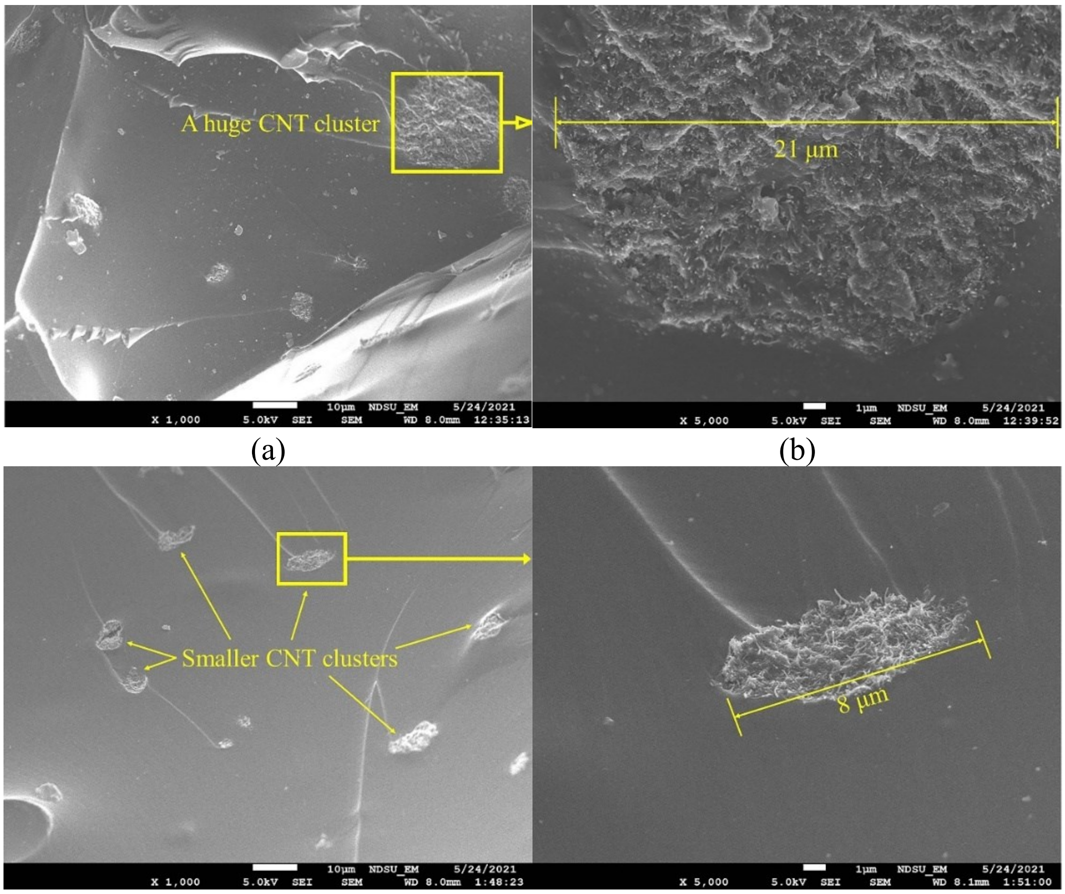

(a) (b)

(c) (d)

Figures 10 Typical CNT clusters on the fracture surfaces of 2% pristine CNTs and CMC/CNT-reinforced epoxy composites: (a) C2; (b) close-view of the CNT cluster of C2; (c); CC2; (d) close-view of the CNT cluster of CC2.

Table 1 SLJ test results

Testing condition	Adhesive material	CNT fraction (%)	Bonding strength (MPa)	STD (%)	Ultimate strain	STD (%)
C0.5	Pristine CNTs	0.5	16.57± 1.12	6.76	1.11 ± 0.084	7.57
CC0.5	CMC treated CNTs	0.5	20.12 ± 1.74	8.65	1.55 ± 0.100	6.45
C1	Pristine CNTs	1	19.21 ± 1.31	6.82	1.40 ± 0.083	5.85
CC1	CMC treated CNTs	1	25.43 ± 1.87	7.35	1.85 ± 0.149	8.01
C2	Pristine CNTs	2	15.85 ± 1.29	8.13	0.91 ± 0.085	9.34
CC2	CMC treated CNTs	2	22.44 ± 1.71	7.62	1.76 ± 0.116	6.59